PO Box 2345, Beijing 100023, China
www.wjgnet.com
wjg@wjgnet.com

World J Gastroenterol 2006 October 21; 12(39): 6376-6381
World Journal of Gastroenterology ISSN 1007-9327

RAPID COMMUNICATION

Dynamic expression of extracellular signal-regulated kinase in rat liver tissue during hepatic fibrogenesis

Xiao-Lan Zhang, Jin-Ming Liu, Chang-Chun Yang, Yi-Lin Zheng, Li Liu, Zhan-Kui Wang, Hui-Qing Jiang

Xiao-Lan Zhang, Jin-Ming Liu, Chang-Chun Yang, Yi-Lin Zheng, Li Liu, Zhan-Kui Wang, Hui-Qing Jiang, Department of Gastroenterology, the Second Hospital of Hebei Medical University, Shijiazhuang 050000, Hebei Province, China
Correspondence to: Professor Xiao-Lan Zhang, Department of Gastroenterology, the Second Hospital of Hebei Medical University, Shijiazhuang 050000, Hebei Province, China. xiaolanzh@126.com
Telephone: +86-311-87222301 Fax: +86-311-87222301
Received: 2006-07-01 Accepted: 2006-07-18

Abstract

AIM: To investigate whether extracellular signal-regulated kinase 1 (ERK_1) is activated and associated with hepatic stellate cell (HSC) proliferation in fibrotic rat liver tissue.

METHODS: Rat hepatic fibrosis was induced by bile duct ligation (BDL). Histopathological changes were evaluated by hematoxylin and eosin staining, and Masson's trichrome method. ERK_1 mRNA in rat liver tissue was determined by reverse transcription-polymerase chain reaction, while the distribution of ERK_1 was assessed by immunohistochemistry. ERK_1 protein was detected by Western blotting analysis. The number of activated HSCs was quantified after alpha smooth muscle actin (α-SMA) staining.

RESULTS: With the development of hepatic fibrosis, the positive staining cells of α-SMA increased obviously, and mainly resided in the portal ducts. Fiber septa and perisinuses were accompanied with proliferating bile ducts. The positive staining areas of the rat livers in model groups 1-4 wk after ligation of common bile duct (12.88% ± 2.63%, 22.65% ± 2.16%, 27.45% ± 1.86%, 35.25% ± 2.34%, respectively) were significantly larger than those in the control group (5.88% ± 1.46%, $P < 0.01$). With the development of hepatic fibrosis, the positive cells of ERK_1 increased a lot, and were mainly distributed in portal ducts, fiber septa around the bile ducts, vascular endothelial cells and perisinusoidal cells. Western blotting analysis displayed that the expression of ERK_1 and ERK_2 protein was up-regulated during the model course, and its level was the highest 4 wk after operation, being 3.9-fold and 7.2-fold higher in fibrotic rat liver than in controls. ERK_1 mRNA was expressed in normal rat livers as well, which was up-regulated two days after BDL and reached the highest 4 wk after BDL. The expression of ERK_1 was positively correlated with α-SMA expression ($r = 0.958$, $P < 0.05$).

CONCLUSION: The expression of ERK_1 protein and mRNA is greatly increased in fibrotic rat liver tissues, which may play a key role in HSC proliferation and hepatic fibrogenesis.

Key words: Extracellular signal-regulated kinase; Hepatic fibrosis; Hepatic stellate cells; Proliferation

Zhang XL, Liu JM, Yang CC, Zheng YL, Liu L, Wang ZK, Jiang HQ. Dynamic expression of extracellular signal-regulated kinase in rat liver tissue during hepatic fibrogenesis. *World J Gastroenterol* 2006; 12(39): 6376-6381

http://www.wjgnet.com/1007-9327/12/6376.asp

INTRODUCTION

Mitogen-activated protein kinase (MAPK) pathway is an important intracellular signal transduction system[1], and extracellular signal-regulated kinase 1 (ERK_1) is the critical and classical pathway of MAPK and plays an important role in several physiological phenomena, including cell local adhesion, migration, proliferation, differentiation, apoptosis and cell cycle[2]. Hepatic stellate cells (HSCs) play a pivotal role in hepatic fibrogenesis[3-6]. In normal liver, HSCs are perisinusoidal mesenchymal elements characterized by intracytoplasmic lipid droplets rich in retinyl esters. On the contrary, in chronic liver injury, HSCs undergo a response known as "activation", which is the transition of quiescent cells into proliferative, fibrogenic and contractile myofibroblasts[7-9].

Up till now, many studies have focused on the role of MAPK in various cultured cells[10,11], little is known about its regulation *in vivo*[12]. No report on dynamic expression of ERK_1 mRNA in fibrotic liver tissue is available. To probe into the molecule mechanism of fibrogenesis by ERK_1, the changes in distribution and contents of ERK_1 protein and mRNA in rat hepatic fibrogenesis were observed by immunohistochemistry, Western blotting and reverse transcription-polymerase chain reaction (RT-PCR). The dynamic expression of α-smooth muscle (α-SMA) as a marker of activated HSCs was also examined by immunohistochemistry in this study.

MATERIALS AND METHODS

Reagents

The monoclonal antibodies against ERK$_1$ and α-SMA were products of Santa Cruz Biotech Inc. Streptavidin-peroxidase immunohistochemical kit was purchased from Zhongshan Biological Technology Co (Beijing). Trizol reagent was obtained from Life Technologies Inc (USA). One tube RT-PCR kit was from Promega Co (USA). Primers for rat ERK$_1$ and β-actin were designed by ourselves in accordance with gene sequence in Genebank, synthesized and purified by Bao Biological Engineering Co (Dalian). All other reagents were analytically pure.

Animal model and experimental protocol

A total of 80 adult male Sprague-Dawley rats weighing 350-400 g were purchased from the Experimental Animal Center of Hebei Medical University (Clearing Grade, Certificate No. 04057). All rats were housed in plastic cages with free access to food and water. The rats were randomly divided into 8 groups (10 rats in each group). The rats were subjected to laparotomy with complete ligation of the common bile duct and received ketamine hydrochloride at a dose of 100 mg/kg by intraperitoneal injection[13]. Under deep anaesthesia, the peritoneal cavity was opened and the common bile duct was double-ligated with 3-0 silk and cut between the ligatures. Control animals underwent a sham operation that consisted of exposure but not ligation of the common bile duct. At various intervals postoperatively, the animals were anaesthetised and the livers were harvested. Liver tissue specimens were routinely fixed in 10% phosphate-buffered formaldehyde and embedded in paraffin. Some liver tissue specimens were used for light microscopy and immunohistochemistry by using anti-α-SMA and ERK$_1$, while others were snap-frozen in liquid nitrogen and stored at -80℃ for RNA analysis. In addition, control livers were harvested 4 wk after sham operation.

Histopathology

Liver specimens were routinely fixed overnight in 10% phosphate-buffered formaldehyde, embedded in paraffin for light microscopic examination. Tissue sections (5-μm thick) were stained with haematoxylin and eosin (H&E) for morphological evaluation and Masson's trichrome for assessment of fibrosis.

Immunohistochemical detection of α-SMA and ERK$_1$

All immunohistochemical studies using the streptavidin-peroxidase technique were performed on 5-μm thick paraformaldehyde-fixed and paraffin-embedded liver tissue sections mounted on APES-coated slides. Slides were deparaffined in xylene and rehydrated in graded ethanol. Endogenous peroxidase activity was quenched with a 3% hydrogen peroxide solution in methanol at room temperature for 30 min, followed by rinsing in pH 6.0 phosphate-buffered saline (PBS). After antigen retrieval in a water bath set in a 10 mmol/L citrate buffer (pH 6.0) at 94℃ for 8 and 10 min, respectively, the slides were immediately cooled for 20 min at room temperature. Non-specific binding sites were blocked by incubation with wash buffer containing 10% normal goat serum at 37℃ for 30 min. The sections were then incubated overnight at 4℃ with a mouse monoclonal antibody directed against α-SMA or a rabbit monoclonal antibody directed against ERK$_1$ at a dilution of 1:100. The secondary antibody bindings were localized using a biotin-conjugated rabbit anti-mouse IgG for α-SMA and goat anti-rabbit IgG for ERK$_1$ (1:100 dilution), followed by incubation with streptavidin-peroxidase complex (1:200 dilution). Peroxidase conjugates were subsequently visualised by utilizing diaminobenzidine (DAB) solution in hydrogen peroxide as a chromogen yielding a brown reaction product. The sections were then counterstained with Mayer's hematoxylin and mounted on a cover slip. All incubations were performed in a moist chamber. Furthermore, between each incubation step, the slides were washed 3 times with PBS for 5 min. To ensure the specificity of antibody, negative control samples were processed in parallel under the same conditions but with omission of the first antibody, which was replaced by an equal volume of PBS. The α-SMA and ERK$_1$ positive parenchymas were measured by a video-image analysis system and expressed as a percentage of area occupied by the signal.

Preparation of cell lysates and Western blotting analysis

Liver tissues from control and bile duct ligation (BDL) animals were quickly removed and washed twice with ice-cold PBS, and then homogenized in modified radioimmunoprecipitation assay (RIPA) buffer (50 mmol/L Tris-HCl, pH 7.5; 150 mmol/L NaCl; 1% Nonident P-40; 0.5% sodium deoxycholate; 0.1% sodium dodecyl sulfate; 1 mmol/L EDTA; 1 mmol/L PMSF; 2 μg/mL l × leupeptin) for 30 min at 4℃, followed by rotating the tubes at 12000 × g at 4℃ for 10 min. After centrifugation, cleared tissue lysates were collected and stored at -80℃ and protein concentration of each sample was determined by Coomassie brilliant blue protein assay. Each sample was adjusted up to a desired protein content of 150 μg, an equal volume of 5 × SDS loading buffer was added and the sample was incubated at 100℃ for 3 min. Lysate containing 150 μg of protein was separated by electrophoresis on 10% acrylamide sodium dodecyl sulfate (SDS) gels and transferred onto nitrocellulose membranes. After blocked in a buffer (pH 7.2) containing 1% bovine serum albumin and 5% skim milk powder, the membranes were incubated with rabbit anti-ERK$_1$ antibodies diluted at 1:600 overnight at 4℃, then incubated for 2 h at 37℃ with horseradish peroxidase-conjugated goat anti-rabbit secondary antibody diluted 1:5000 in a blocking buffer. After washed 3 times with PBS containing 0.1% Tween 20, immunoreactive proteins were visualized with an enhanced chemiluminescence detection system on radiograph film. The intensity of the bands was determined by scanning video densitometry. Experiments were performed at least 3 times with similar results.

RNA extraction and RT-PCR assay

Expression of ERK$_1$ mRNA was evaluated by RT-PCR. Total RNA from liver specimens (100 mg) was isolated using a monophasic solution of phenol and guanidine thiocyanate (Trizol), precipitated in ethanol and resuspended in sterile RNAase-free water for storage at -80℃ until use, as recommended by the suppliers. Total

RNA was quantified spectrometrically at 260 nm, and the quality of isolated RNA was analysed on agarose gels under standard conditions. One-step RT-PCR was performed according to the manufacturer's instructions. Two-microgram RNA was added to each reaction and RT-PCR was routinely performed utilizing 5 units of AMV reverse transcriptase, 5 units of *Tfl* DNA polymerase, 10 pmol of each oligonucleotide primer, 10 pmol of dNTP mix and 25 mmol/L $MgSO_4$ in a final reaction volume of 50 μL. Primer sequences were as follows: ERK_1 : forward 5' - GCT GAC CCT GAG CAC GAC CA -3' and reverse 5'- CTG GTT CAT CTG TCG GAT CA -3', fragment length 451 bp; β-actin: forward 5'- AGC TGA GAG GGA AAT CGT GCG -3' and reverse 5'- GTG CCA CCA GAC AGC ACT GTG -3', fragment length 300 bp. RT-PCR was performed in the following steps: reverse transcription at 41℃ for 45 min, pre-denaturation at 94℃ for 2 min. Then amplification was performed in a thermal controller for 35 cycles (denaturation at 94℃ for 40 s, annealing at 52℃ for 1 min, extension at 72℃ for 1.5 min, and a final extension at 72℃ for 10 min). Ten μL of the PCR products was analyzed by 1.5% agarose gel electrophoresis with TAE buffer at 80 V for 40 min, visualized with ethidium bromide staining and photographed under UV illumination. The band intensities were quantified by densitometry. ERK_1/β-actin quotient was the indication of ERK_1. Experiments were performed at least 3 times with similar results.

Statistical analysis

The data were expressed as mean ± SD. Group means were compared by using analysis of variance followed by the Student-Newman-Keuls test if the former was significant. The correlation between the expressions of ERK_1 and α-SMA was analyzed for statistical significance by the simple linear regression analysis. $P < 0.05$ was considered statistically significant.

RESULTS

Histology of progressive fibrotic liver injury

In the present study, spotted (or scattered) perivenular degeneration of hepatocytes, increased inflammatory infiltrate in the necrotic areas and bile ductular proliferation in the portal triads were observed after 1 wk of BDL. After 2 wk of BDL, all rats showed expanded portal tracts with fibrous tissue, portal-to-portal fibrous bridging, nodular transformation and widespread proliferating bile ductules which extended into the parenchyma in places, without clear-cut cirrhosis. After 3-4 wk of BDL, the animals developed severe fibrosis associated with proliferating bile ducts which formed a continuous meshwork of connective tissue with complete distortion of lobular architecture, whereas there was no histological abnormality or evidence of stainable collagen in any of the sham-operated control livers.

Identification of proliferating and activated HSCs

Immunostaining for α-SMA was used to detect and quantify the number of activated HSCs in this study. The α-SMA positive cells in the sham-operated control livers were observed in vascular smooth muscle cells and sinusoids with a weak staining. With the development of hepatic fibrosis, the number of positive α-SMA cells was greatly elevated and mainly resided in the cells of portal ducts, fiber septa, and perisinuses accompanied with proliferating bile ducts. The positive areas of the rat livers were larger in model groups at 1 to 4 wk (12.88 % ± 2.63%, 22.65% ± 2.16%, 27.45% ± 1.86%, 35.25% ± 2.34%) than in control group (5.88% ± 1.46%) ($P < 0.01$, Figure 1A-1C).

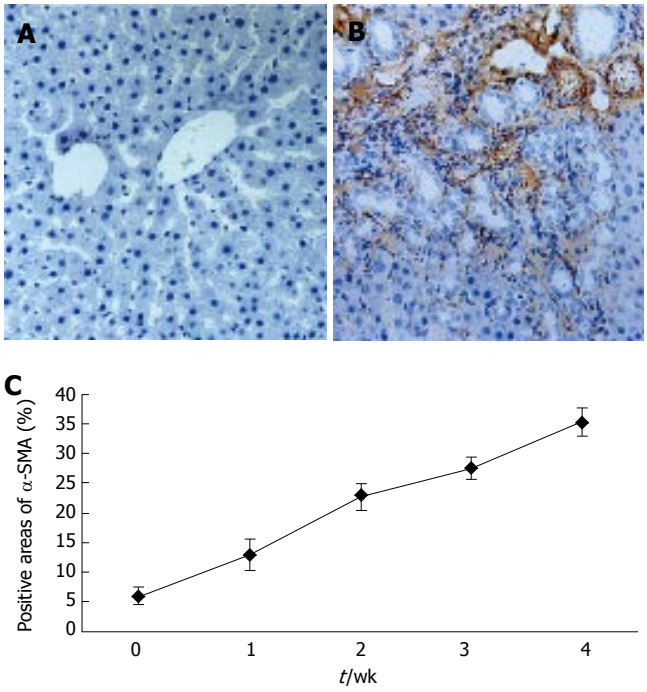

Figure 1 α-SMA protein expression in immunohistochemically-stained liver tissue (SP × 200). **A**: Few α-SMA expressions in sham operation group; **B**: Positive α-SMA cells residing in the cells of portal ducts, fiber septa, perisinuses and around the proliferated bile ducts 2 wk after BDL; **C**: Positive areas of α-SMA expression in model groups at wk 1 to 4 after common bile duct ligation.

Distribution of ERK_1 protein in bile duct-ligated rat liver tissues

To explore the distribution of ERK_1, the normal and fibrotic rat liver tissue sections were immunostained using specific monoclonal anti-ERK_1 antibody. ERK_1 was found in vascular endothelial and perisinusoidal cells of normal rat liver tissue sections. With the development of hepatic fibrosis, the positive ERK_1 cells increased a lot and were mainly distributed in portal ducts, fiber septa, around the bile ducts, as well as in vascular endothelial and perisinusoidal cells and hepatocytes. ERK_1 protein was expressed not only in cytoplasm mentioned above, but also in nuclear membrane, indicating its activation. The positive areas of rat livers in model groups at 1 to 4 wk (9.58% ± 1.01%, 17.43% ± 1.78%, 23.88% ± 2.97%, 28.63% ± 2.72%) were larger than those in control group (5.03% ± 1.10%) ($P < 0.01$, Figure 2A-2C).

Expression of ERK_1 protein in common bile duct-ligated rat livers

Western blot analysis showed that ERK_1 was expressed in normal rats with a prolonged model-making period.

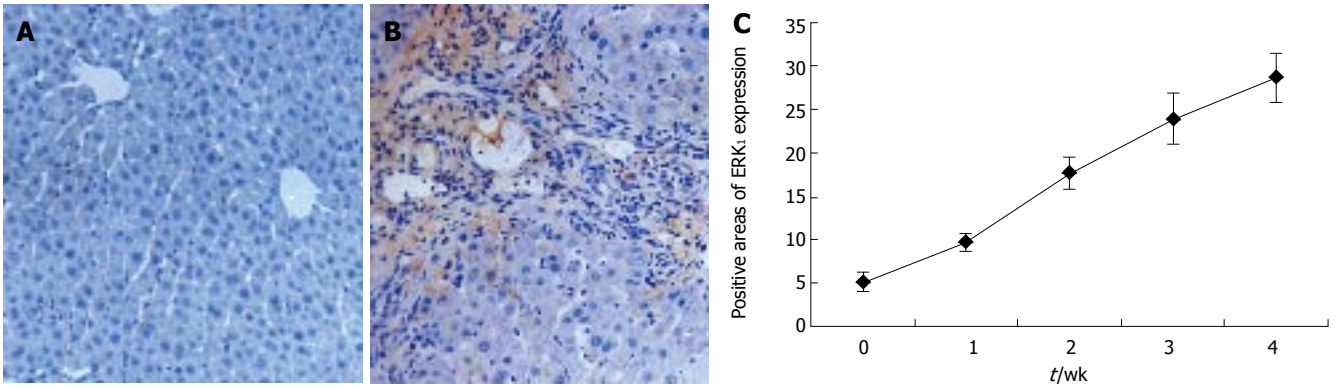

Figure 2 ERK1 distribution in immunohistochemically-stained liver tissue (SP × 200). **A**: ERK1 distribution in sham operation group; **B**: ERK1 distribution 2 wk after BDL; **C**: The time course of ERK1 distribution in hepatic fibrogenesis.

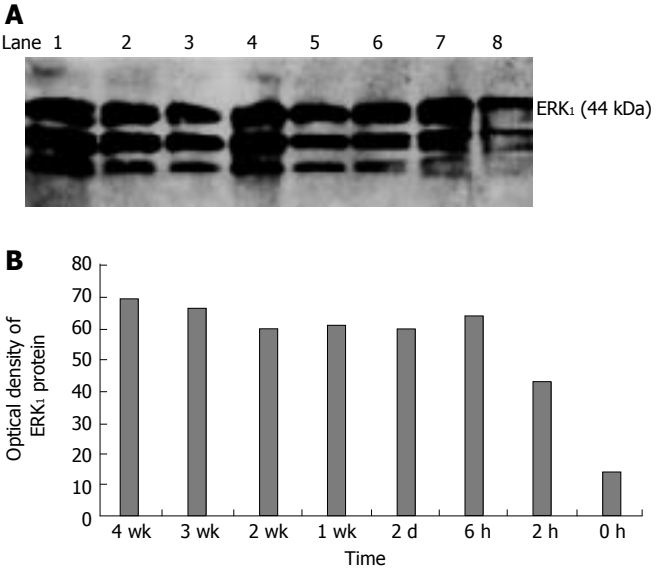

Figure 3 Time course of ERK1 protein expression (**A**) and quantitative results (**B**) in fibrotic and normal rat liver tissues by Western blotting analysis. 1: 4 wk after BDL; 2: 3 wk after BDL; 3: 2 wk after BDL; 4: 1 wk after BDL; 5: 2 d after BDL; 6: 6 h after BDL; 7: 2 h after BDL; 8: Sham operation group.

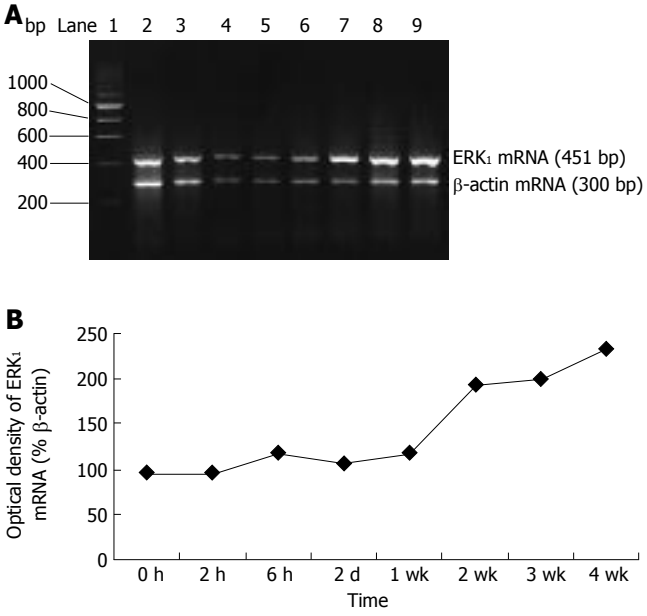

Figure 4 Electrophoresis of RT-PCR for ERK1 mRNA expression in hepatic fibrogenesis at different time points (**A**) and percentage of optical density of ERK1 mRNA electrophoretic strip (**B**). 1: marker; 2: sham operation group; 3: 2 h after BDL; 4: 6 h after BDL; 5: 2 d after BDL; 6: 1 wk after BDL; 7: 2 wk after BDL; 8: 3 wk after BDL; 9: 4 wk after BDL.

The expression of ERK1 increased 3.07-, 4.51-, 4.36-, 4.36-, 4.36- and 4.71-fold at 2, 6 h; 2 d; 1, 2 and 3 wk; respectively, and reached the peak at 4 wk, which was 4.93 times of the expression in sham-operated group ($P < 0.01$, Figure 3A and 3B).

Increased ERK1 mRNA expression in bile duct-ligated rat livers

Although ERK1 protein is produced by liver tissue *in vivo*, it is not clear whether the ERK1 mRNA level under fibrogenic response is increased *in vivo*. Therefore, we investigated the production of ERK1 mRNA in liver. Total liver RNA was analyzed by RT-PCR. The results revealed faint transcript of ERK1 mRNA in sham-operated rat livers. However, specific banding to ERK1 mRNA was detected in fibrotic liver sections. Moreover, ERK1 mRNA expression was initially up-regulated at 6 h and reached its peak level 4 wk after BDL, which increased 2.4-fold. Levels of the housekeeping gene, β-actin, did not show any significant differences between control and BDL rat liver tissue (Figure 4A and 4B).

Analysis of relation between ERK1 and α-SMA

Immunohistochemistry experiments were performed to analyze whether the above described ERK1 protein distribution was correlated with α-SMA in sham operated livers compared with BDL rats. The results indicated that ERK1 was positively correlated with α-SMA ($r = 0.958$, $P < 0.05$).

DISCUSSION

HSCs, the principal cellular source of extracellular matrix during chronic liver injury, undergo a transition into α-SMA-expressing myofibroblastlike cells in

response to various liver injuries such as ECM, cytokine, inflammation mediator, ethanal, oxygen radical and lactic acid. Furthermore, HSC activation is associated with stellate cell proliferation, increased contractility and enhanced matrix production. HSCs express a number of fibrogenic and proliferative cytokines and their cognate receptors. Therefore, HSCs play a crucial role in cellular and molecular events that lead to hepatic fibrosis[4]. Cassiman *et al*[13] and Ramm *et al*[14] have demonstrated that positive α-SMA cells mainly reside in the portal ducts and fiber septa, accompanied with proliferating tubercle, corresponding to the distribution of collagen. This study displayed that with the development of hepatic fibrosis, the positive α-SMA cells were greatly elevated and mainly situated in cells of the portal ducts, fiber septa, perisinuses accompanied with proliferating bile ducts. The positive areas of α-SMA in rat livers of model groups at 1 to 4 wk increased in turn and were larger than those in control group ($P < 0.01$). The result is in accordance with the above reports and indicates that the level of liver fibrosis can respond to α-SMA.

The activation and proliferation of HSCs may be regulated by various factors and signal transduction pathways[7,15]. MAPK is a group of cytoplasmic serine/threonine kinases distributed extensively in cytoplasm, as a point of convergence of extracelluar signal causing nuclear reaction[1]. It becomes activated after threonine and tyrosine are phosphorylated altogether. In the MAPK family, ERK has been identified. ERK subset includes 2 subtypes: ERK_1 ($P44^{MAPK}$) and ERK_2 ($P42^{MAPK}$). The activation pathway is RAS-RAF-MEK-ERK. The combination of extracellular stimulation signal and receptors in cell membrane provokes dimerization of receptors and then phosphorylates self residue-Tyr. Some adapter proteins such as (growth factor receptor $bound_2$ (Grb_2) are recruited. Grb_2 is composed of one SH_2 region and two SH_3 regions. The SH_3 region of Grb_2 can combine with son of sevenless, which provocates the change of Ras's GDP and GTP. RAS activates RAF kinases further and phosphorylated RAF activates mitogen-activated protein kinase kinase (MEK), which can phosphorylate Thr and Tyr residues of $ERK_{1/2}$. At last, activated ERK enters nuclear membrane to regulate gene transcription and provokes cell biologic effects.

The role of ERK in promoting HSC proliferation *in vitro* has been increasingly acquainted in recent years. As mentioned earlier, it has been suggested that many cytokines, such as platelet derived growth factor (PDGF), endothelin (ET), epidermal growth factor (EGF), insulin, insulin-like growth factor-1 (IGF-1) and tumor necrosis factor (TNF), as well as endotoxin, ethanol, acetaldehyde, ROS and ECM, can all activate HSCs and promote the prodution of ERK[10,16-19]. PD98059, an inhibitor of MEK kinase which is a upstream signal molecule of ERK, can restrain the transformation of HSCs into myofibroblasts, HSC proliferation and collagen synthesis[14, 20-22]. The study on HSC-deleting MAPK gene *in vitro* discovered that the collagen gene expression of HSCs decreases to one third of the primary[23]. On the contrary, little is known about the role and regulation mechanism of ERK *in vivo*. In addition, the mechanism of ERK mRNA is unknown. Nguyen *et al*[24] have demonstrated that the expression of ERK_1 and ERK_2 in patients with alcoholic liver disease increases 3.9- and 3.2-fold respectively, compared with that in normal people. By using immunohistochemistry, Alvaro *et al*[25] have confirmed that the activated $ERK_{1/2}$ in rat liver enters nuclear membrane from cytoplasm, and the expression coincides with liver pathology, suggesting that ERK_1 protein and ERK_1 mRNA are scarcely expressed in normal rat livers. In addition, ERK_1 protein and ERK_1 mRNA expressions are elevated with the progression of hepatic fibrosis. The position distribution demonstrates that ERK_1 protein is scarcely expressed in vascular endothelial and perisinusoidal cells in normal rat liver. With the development of hepatic fibrosis, the positive ERK_1 cells are mainly resided along with HSCs, in portal ducts, fibrotic septa, and epithelium of bile ducts. ERK_1 protein is expressed not only in plasma of cells, but also in nuclearmembrane, indicating its activation. Based on these results, we presume that hepatocytes, vascular endothelial cells, epithelium of bile ducts and HSCs are all cellular sources of ERK_1. However, the major cellular source is HSCs during hepatic fibrosis. ERK_1 in the MAPK family probably participates in the development of hepatic fibrogenesis.

In conclusion, ERK_1 protein distribution is positively correlated with α-SMA. ERK_1 is associated with HSC proliferation. Activation of ERK_1 in rat liver tissue can activate the downstream signal molecule which modulates gene expression of HSCs and gives rise to hepatic fibrosis.

REFERENCES

1 **Boudreau NJ**, Jones PL. Extracellular matrix and integrin signalling: the shape of things to come. *Biochem J* 1999; **339** (Pt 3): 481-488

2 **Gentilini A**, Marra F, Gentilini P, Pinzani M. Phosphatidylinositol-3 kinase and extracellular signal-regulated kinase mediate the chemotactic and mitogenic effects of insulin-like growth factor-I in human hepatic stellate cells. *J Hepatol* 2000; **32**: 227-234

3 **Friedman SL**. Molecular mechanisms of hepatic fibrosis and principles of therapy. *J Gastroenterol* 1997; **32**: 424-430

4 **Friedman SL**. Cytokines and fibrogenesis. *Semin Liver Dis* 1999; **19**: 129-140

5 **Pinzani M**, Marra F, Carloni V. Signal transduction in hepatic stellate cells. *Liver* 1998; **18**: 2-13

6 **Liu XJ**, Yang L, Luo FM, Wu HB, Qiang Q. Association of differentially expressed genes with activation of mouse hepatic stellate cells by high-density cDNA microarray. *World J Gastroenterol* 2004; **10**: 1600-1607

7 **Iredale JP**. Hepatic stellate cell behavior during resolution of liver injury. *Semin Liver Dis* 2001; **21**: 427-436

8 **Jiang HQ**, Zhang XL. Progress in the study of pathogenesis in hepatic fibrosis. *Shijie Huaren Xiaohua Zazhi* 2000; **8**: 687-689

9 **Gressner AM**. The cell biology of liver fibrogenesis-an imbalance of proliferation, growth arrest and apoptosis of myofibroblasts. *Cell Tissue Res* 1998; **292**: 447-452

10 **Poulos JE**, Weber JD, Bellezzo JM, Di Bisceglie AM, Britton RS, Bacon BR, Baldassare JJ. Fibronectin and cytokines increase JNK, ERK, AP-1 activity, and transin gene expression in rat hepatic stellate cells. *Am J Physiol* 1997; **273**: G804-G811

11 **Talarmin H**, Rescan C, Cariou S, Glaise D, Zanninelli G, Bilodeau M, Loyer P, Guguen-Guillouzo C, Baffet G. The mitogen-activated protein kinase kinase/extracellular signal-regulated kinase cascade activation is a key signalling pathway involved in the regulation of G(1) phase progression in proliferating hepatocytes. *Mol Cell Biol* 1999; **19**: 6003-6011

12 **Nishio H**, Kuwabara H, Mori H, Suzuki K. Repeated fasting stress causes activation of mitogen-activated protein kinases (ERK/JNK) in rat liver. *Hepatology* 2002; **36**: 72-80

13 **Cassiman D**, Libbrecht L, Desmet V, Denef C, Roskams T. Hepatic stellate cell/myofibroblast subpopulations in fibrotic human and rat livers. *J Hepatol* 2002; **36**: 200-209
14 **Ramm GA**, Carr SC, Bridle KR, Li L, Britton RS, Crawford DH, Vogler CA, Bacon BR, Tracy TF. Morphology of liver repair following cholestatic liver injury: resolution of ductal hyperplasia, matrix deposition and regression of myofibroblasts. *Liver* 2000; **20**: 387-396
15 **Guo CY**, Wu JY, Wu YB, Zhong MZ, Lu HM. Effects of endothelin-1 on hepatic stellate cell proliferation, collagen synthesis and secretion, intracellular free calcium concentration. *World J Gastroenterol* 2004; **10**: 2697-2700
16 **Marra F**, Arrighi MC, Fazi M, Caligiuri A, Pinzani M, Romanelli RG, Efsen E, Laffi G, Gentilini P. Extracellular signal-regulated kinase activation differentially regulates platelet-derived growth factor's actions in hepatic stellate cells, and is induced by *in vivo* liver injury in the rat. *Hepatology* 1999; **30**: 951-958
17 **Reeves HL**, Thompson MG, Dack CL, Burt AD, Day CP. The role of phosphatidic acid in platelet-derived growth factor-induced proliferation of rat hepatic stellate cells. *Hepatology* 2000; **31**: 95-100
18 **Carloni V**, Defranco RM, Caligiuri A, Gentilini A, Sciammetta SC, Baldi E, Lottini B, Gentilini P, Pinzani M. Cell adhesion regulates platelet-derived growth factor-induced MAP kinase and PI-3 kinase activation in stellate cells. *Hepatology* 2002; **36**: 582-591
19 **Takashima T**, Kawada N, Maeda N, Okuyama H, Uyama N, Seki S, Arakawa T. Pepstatin A attenuates the inhibitory effect of N-acetyl-L-cysteine on proliferation of hepatic myofibroblasts (stellate cells). *Eur J Pharmacol* 2002; **451**: 265-270
20 **Sohara N**, Trojanowska M, Reuben A. Oncostatin M stimulates tissue inhibitor of metalloproteinase-1 via a MEK-sensitive mechanism in human myofibroblasts. *J Hepatol* 2002; **36**: 191-199
21 **Svegliati-Baroni G**, Ridolfi F, Di Sario A, Casini A, Marucci L, Gaggiotti G, Orlandoni P, Macarri G, Perego L, Benedetti A, Folli F. Insulin and insulin-like growth factor-1 stimulate proliferation and type I collagen accumulation by human hepatic stellate cells: differential effects on signal transduction pathways. *Hepatology* 1999; **29**: 1743-1751
22 **Svegliati-Baroni G**, Ridolfi F, Di Sario A, Saccomanno S, Bendia E, Benedetti A, Greenwel P. Intracellular signaling pathways involved in acetaldehyde-induced collagen and fibronectin gene expression in human hepatic stellate cells. *Hepatology* 2001; **33**: 1130-1140
23 **Davis BH**, Chen A, Beno DW. Raf and mitogen-activated protein kinase regulate stellate cell collagen gene expression. *J Biol Chem* 1996; **271**: 11039-11042
24 **Nguyen VA**, Gao B. Expression of interferon alfa signaling components in human alcoholic liver disease. *Hepatology* 2002; **35**: 425-432
25 **Alvaro D**, Onori P, Metalli VD, Svegliati-Baroni G, Folli F, Franchitto A, Alpini G, Mancino MG, Attili AF, Gaudio E. Intracellular pathways mediating estrogen-induced cholangiocyte proliferation in the rat. *Hepatology* 2002; **36**: 297-304

S- Editor Liu Y **L- Editor** Wang XL **E- Editor** Bi L